Isomer studies in the vicinity of the doubly-magic nucleus ^{100}Sn: Observation of a new low-lying isomeric state in ^{97}Ag

Christine Hornung, Daler Amanbayev, Irene Dedes, Gabriella Kripko-Koncz, Ivan Miskun, Noritaka Shimizu, Samuel Ayet San Andrés, Julian Bergmann, Timo Dickel, Jerzy Dudek, et al.

▶ **To cite this version:**

Christine Hornung, Daler Amanbayev, Irene Dedes, Gabriella Kripko-Koncz, Ivan Miskun, et al.. Isomer studies in the vicinity of the doubly-magic nucleus ^{100}Sn: Observation of a new low-lying isomeric state in ^{97}Ag. Phys.Lett.B, 2020, 802, pp.135200. 10.1016/j.physletb.2020.135200 . hal-02475267

HAL Id: hal-02475267
https://hal.science/hal-02475267

Submitted on 22 Jul 2020

HAL is a multi-disciplinary open access archive for the deposit and dissemination of scientific research documents, whether they are published or not. The documents may come from teaching and research institutions in France or abroad, or from public or private research centers.

L'archive ouverte pluridisciplinaire **HAL**, est destinée au dépôt et à la diffusion de documents scientifiques de niveau recherche, publiés ou non, émanant des établissements d'enseignement et de recherche français ou étrangers, des laboratoires publics ou privés.

Isomer Studies in the Vicinity of the Doubly-Magic Nucleus ^{100}Sn: Observation of a New Low-Lying Isomeric State in ^{97}Ag

Christine Hornung[a,], Daler Amanbayev[a], Irene Dedes[b], Gabriella Kripko-Koncz[a], Ivan Miskun[a], Noritaka Shimizu[c], Samuel Ayet San Andrés[a,d], Julian Bergmann[a], Timo Dickel[a,d], Jerzy Dudek[e,b], Jens Ebert[a], Hans Geissel[a,d], Magdalena Górska[d], Hubert Grawe[d], Florian Greiner[a], Emma Haettner[d], Takaharu Otsuka[f], Wolfgang R. Plaß[a,d], Sivaji Purushothaman[d], Ann-Kathrin Rink[a], Christoph Scheidenberger[a,d], Helmut Weick[d], Soumya Bagchi[a,d,g], Andrey Blazhev[h], Olga Charviakova[i], Dominique Curien[e], Andrew Finlay[j], Satbir Kaur[g], Wayne Lippert[a], Jan-Hendrik Otto[a], Zygmunt Patyk[i], Stephane Pietri[d], Yoshiki K. Tanaka[d], Yusuke Tsunoda[c], John S. Winfield[d]

[a] *II. Physikalisches Institut, Justus-Liebig-Universität Gießen, 35392 Gießen, Germany*
[b] *Institute of Physics, Marie Curie-Sklodowska University, PL-20 031 Lublin, Poland*
[c] *Center for Nuclear Study, University of Tokyo, Hongo, Bunkyo-ku, Tokyo 113-0033, Japan*
[d] *GSI Helmholtzzentrum für Schwerionenforschung GmbH, 64291 Darmstadt, Germany*
[e] *Université de Strasbourg, CNRS, IPHC UMR 7178, F-67 000 Strasbourg, France*
[f] *RIKEN Nishina Center, 2-1 Hirosawa, Wako, Saitama 351-0198, Japan*
[g] *Saint Mary's University, NS B3H 3C3 Halifax, Canada*
[h] *Institut für Kernphysik, Universität zu Köln, D-50937 Köln, Germany*
[i] *National Centre for Nuclear Research, Hoża 69, 00-681 Warszawa, Poland*
[j] *TRIUMF, BC V6T 2A3 Vancouver, Canada*

Abstract

Long-lived isomeric states in ^{97}Ag and $^{101-109}$In were investigated with the FRS Ion Catcher at GSI. In the isotope ^{97}Ag, a long-lived $\left(1/2^{-}\right)$ isomeric state was discovered, and its excitation energy was determined to be 618(38) keV. This is simultaneously the first discovery of a nuclear isomeric state by multiple-reflection time-of-flight mass spectrometry. The measured excitation energies were compared to large-scale shell-model calculations, which indicated the importance of core excitation around ^{100}Sn. Furthermore, advanced mean-field calculations for the ^{97}Ag nucleus and relevant neighboring nuclei were performed, which contributed to a better understanding of the repetitive appearance of certain isomeric structures in neighboring nuclei, and supported the discovery of the isomeric state in ^{97}Ag in a global shell-evolution scheme.

Keywords: mass spectrometry, multiple-reflection time-of-flight mass spectrometry, nuclear structure, isomers, isomer-to-ground state ratio, exotic nuclei

1. Introduction

The lifetimes of isomers are much longer than those of common excited states [1]. There are several reasons for this: the shape, the spin, or the spin orientation relative to a symmetry axis of the isomeric state. The properties of nuclear isomers [2] are significant for the understanding of nuclear structure because they provide stringent tests for nuclear models. There is a broad field

of applications for nuclear isomers, ranging from new possibilities for the storage of energy to the impact on nuclear astrophysics and the synthesis of the elements in the universe [3].

The nucleus ^{100}Sn is the heaviest self-conjugate doubly-magic nucleus in the chart of nuclides, and therefore, attracts a broad interest in both experimental and theoretical nuclear physics. Since its discovery [4, 5], it has been the subject of many investigations and measurements, leading to a better understanding of the nuclear structure in this region of the nuclear chart [6]. Because the experimental access to ^{100}Sn is still limited, most of the data obtained stems from nuclei in the neighborhood. Therefore, the knowledge of their detailed structure is indispensable in understanding this region of the chart of nuclides. Recently, new isotopes in this region were identified, and their half-lives and decay properties have been measured [7–10]. In-beam and decay spectroscopy delivered new information on single particle level energies and residual nucleon-nucleon interaction [6], especially below ^{100}Sn, in the last 20 years. ^{100}Sn, as an open spin-orbit (SO) core nucleus, allows the study of the $1g_{9/2}$ intruder-dominated states, with significantly different angular momentum from that of the neighboring states. Consequently, states that are close in energy have a large difference in spin, causing the existence of long-lived isomeric states, i.e., meta-stable states. The comparison of large scale shell model (LSSM) and mean field approaches, and their complementarity, will lead to a clearer understanding of nuclear structure evolution in this region.

The masses of nuclei reflect their total binding energy, and can be measured directly using mass spectrometry techniques. The mass reveals basic information about nuclear properties [11]. Despite experimental efforts, documented by many Penning trap measurements [12–15], there is a large uncertainty still associated with the mass of ^{100}Sn ($\Delta m \approx 300$ keV) [16, 17]. The heaviest $N = Z$ nuclides with a mass that is measured directly is ^{76}Sr. Those neutron-deficient nuclei are synthesized in astrophysical environments, where the rapid proton capture process (rp-process) takes place [18, 19]. The modeling of the rp-process is necessary in understanding the origin of the elements and the abundances of the isotopes in the universe.

High-resolution mass spectrometry is a relatively new tool to study isomeric states. During the last two decades, isomeric states were discovered by mass measurements, using storage rings [20, 21] and Penning traps [22]. The half-lives are difficult to access in the millisecond range because established high-resolution mass spectrometry methods are either not fast enough, or have very limited mass ranges that can be simultaneously measured. For decay spectroscopy, the challenge is the requirement of long coincident-times, which result in a strongly increased background. The first discovery of a nuclear isomeric state, by multiple-reflection time-of-flight mass spectrometry, is presented in this paper. The multiple-reflection time-of-flight mass spectrometer (MR-TOF-MS) of the FRS Ion Catcher [23] is, due to its unique combination of performance parameters, the ideal device for the search for new isomeric states [24]. It combines a high mass resolving power ($m/\Delta m > 600,000$), short measurement time (> 0.01 s), high accuracy (relative mass accuracy of $< 10^{-7}$), and non-scanning operation. Combined with a gas-filled stopping cell, it is applicable for production methods at the Coulomb barrier and relativistic energies. Therefore, the MR-TOF-MS of the FRS Ion Catcher has a high discovery potential for isomeric states with half-lives as low as the ms region.

2. Experiment

The FRS Ion Catcher [25] is installed, at the final focal plane of the fragment separator FRS [26] at GSI. The FRS Ion Catcher consists of three main parts: (i) the gas-filled cryogenic stopping cell (CSC) [27–30], which executes the complete slowing-down of the exotic nuclei

produced at relativistic energies, (ii) a radio frequency quadrupole (RFQ) beamline [30–33], which is used for mass-selective transport and differential pumping, and (iii) the MR-TOF-MS [23, 34, 35], which performs direct mass measurements.

In this experiment, the exotic nuclei and their isomeric states were produced via projectile fragmentation, using a 600 MeV/u ^{124}Xe projectile beam on a beryllium production target, with an areal density of 1.622 g/cm^2. The intensity was approximately 3×10^8 ions per second, with a typical spill length of 500 ms and a spill period of approximately 4 s. The mono-energetic degrader at the central focal plane [36] had an areal density of 737.1 mg/cm^2. The CSC had an areal density of 4.6±0.15 mg/cm^2 helium, corresponding to a pressure of 75 mbar, at a temperature of 82 K. The extraction time for this experiment was approximately 200 ms [37]. The molecular background, generated in the CSC, was suppressed in the RFQ beamline by the isolation-dissociation-isolation method [38].

The measurements, in the MR-TOF-MS, were performed with a time-of-flight of approximately 19 ms (typically about 600 isochronous turns in the analyzer) and a mass resolving power of up to 450,000. The mono-energetic degrader, at the mid-focal plane, of the FRS ensured that the isotopes had only a narrow range distribution; this feature was used as an additional identification tool [39]. The measurements were done using different settings of the aluminum degrader, at the final focal plane of the FRS. In addition, a measurement with one more turn in the time-of-flight analyzer, was performed. This measurement, which had a different number of reflections, served as further confirmation of the particle identification [40].

The details of the MR-TOF-MS data-analysis procedure were reported in a separate publication [40]. The procedure allowed accurate mass determination, even in the most challenging conditions, including very low numbers of events and overlapping mass distributions. In the mass measurements reported in Ref. [40], a relative uncertainty as low as 6×10^{-8}, was achieved. Further details on the experiment and the data evaluation employed for the nuclides reported here, and their isomeric states, are provided in Ref. [39, 41].

3. Experimental Results

The mass-to-charge spectrum for $^{101g,m}\mathrm{In}^+$ ions in the ground and isomeric state, measured with the MR-TOF-MS, is shown in Fig. 1. The ground and isomeric states were fitted with a so-called double hyper-EMG [44] (red line for $^{101g}\mathrm{In}^+$ and blue line for $^{101m}\mathrm{In}^+$) with one exponential tail on both sides. The peak shape was determined from a high statistical peak. For the isomeric state, 9 counts were detected. The background in the spectrum was 1 count per 3 FWHM.The estimated spins of the ground and isomeric states were $\left(9/2^+\right)$ and $\left(1/2^-\right)$, respectively. This was the first mass measurement for the isotope ^{101}In. A mass excess value for the ground state was determined to be -68535(20) keV for ^{101}In. The extrapolated value in the AME 2016 [16] is -68610(200) keV. Our measured value is expected to have an impact on the nucleosynthesis in the *rp*-process [45]. The excitation energy of the $\left(1/2^-\right)$ isomeric state was determined to be 608(57) keV. The $\left(1/2^-\right)$ isomeric state of ^{101}In was recently confirmed by an isochronous mass spectrometry measurement at the HIRFL-CSR facility in Lanzhou [46]. An excitation energy of 659(50) keV was reported, which is in agreement with the result presented in this paper.

The nucleus ^{101}In was produced in fragmentation, with a production cross section of 230 nbarn [47]. An isomer-to-ground state ratio of 0.14 ± 0.03 was measured. Therefore, an effective production cross section, of approximately 30 nbarn, can be deduced for the isomeric state. This

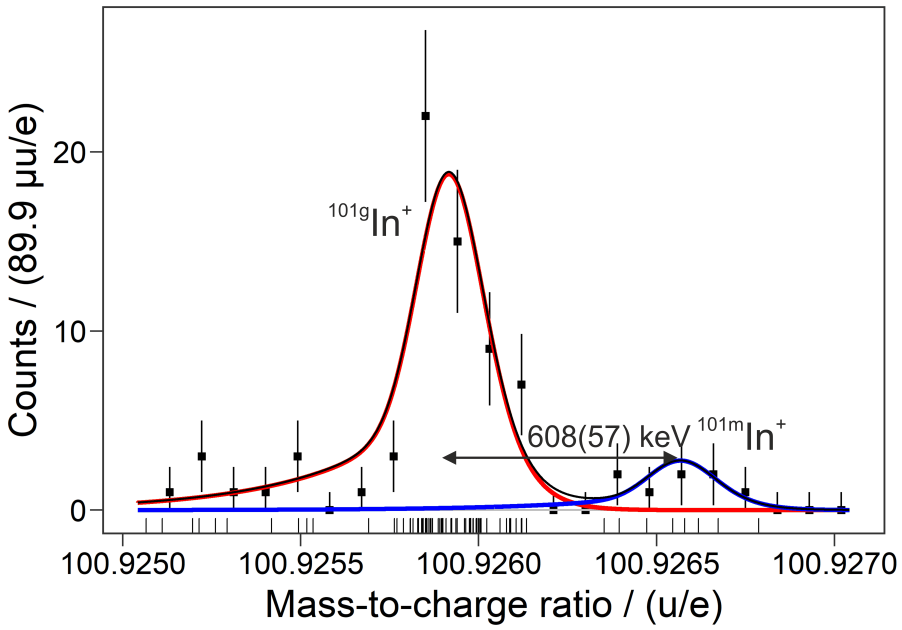

Figure 1: Measured mass-to-charge spectrum of $^{101}In^{+}$ ions. The fit of the ground state and the $\left(1/2^{-}\right)$ isomeric state are shown by the red and blue line, respectively. The histogram of the measured spectrum is drawn only to guide the eye. The evaluation was based on measured unbinned data ("rug" graph below the histogram).

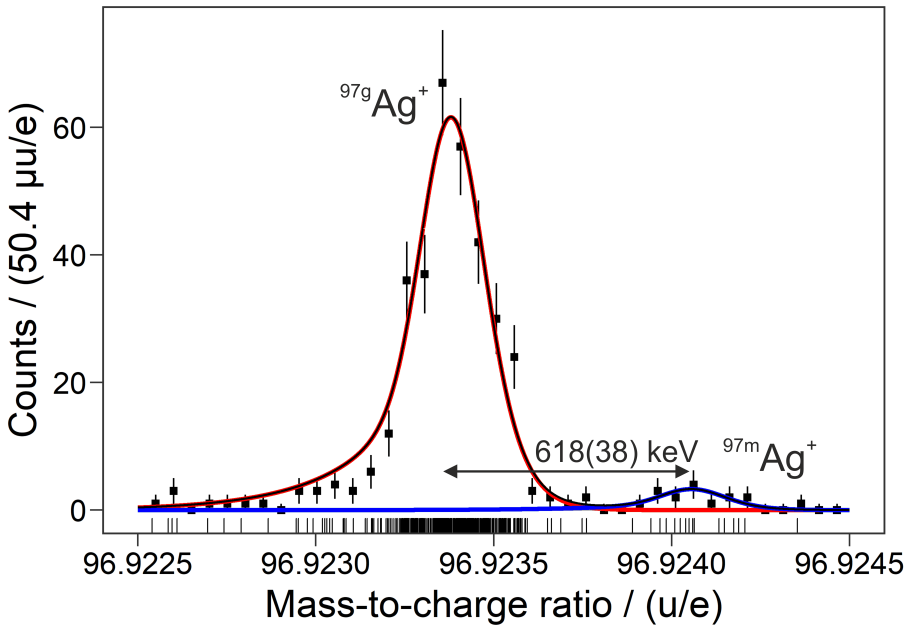

Figure 2: Measured mass-to-charge spectrum of $^{97}Ag^{+}$ ions. The fit of the ground state and the $\left(1/2^{-}\right)$ isomeric state are shown by the red and blue line, respectively. The histogram of the measured spectrum is drawn only to guide the eye. The evaluation was based on measured unbinned data ("rug" graph below the histogram).

Nuclide	Half-life	ME_{FRS-IC} [keV]	ME_{Lit} [keV]	ME_{FRS-IC} - ME_{Lit} [keV]
^{97}Ag	(25.5 ± 0.3) s	-70904 ± 12	-70830 ± 110	-74 ± 111
^{101}In	(15.1 ± 1.1) s	-68535 ± 20	-68610 ± 200 #	75 ± 201
^{103}In	(60 ± 1) s	-74631 ± 25	-74633 ± 10	2 ± 27
^{105}In	(5.07 ± 0.07) m	-79677 ± 31	-79641 ± 10	-36 ± 33
^{107}In	(32.4 ± 0.3) m	-83593 ± 27	-83564 ± 11	-19 ± 29
^{109}In	(4.167 ± 0.018) h	-86522 ± 34	-86490 ± 4	-32 ± 34

Nuclide	Half-life	$E_{exc,FRS-IC}$ [keV]	$E_{exc,Lit}$ [keV]	$E_{exc,FRS-IC}$ - $E_{exc,Lit}$ [keV]
^{97m}Ag	100 ms #	618 ± 38	400 ± 200 #	218 ± 204
^{101m}In	10 s #	608 ± 57	550 ± 100 #	58 ± 115
^{103m}In	(34 ± 2) s	689 ± 77	631.7 ± 0.1	57 ± 77
^{105m}In	(48 ± 6) s	702 ± 27	674.08 ± 0.25	28 ± 27
^{107m}In	(50.4 ± 0.6) s	663 ± 22	678.5 ± 0.3	-16 ± 22
^{109m}In	(1.34 ± 0.07) m	651 ± 27	650.1 ± 0.3	1 ± 27
^{109n}In	(209 ± 6) ms	2098 ± 11	2101.8 ± 0.2	4 ± 11

Table 1: Measured mass excess (ME_{FRS-IC}) values of the ground states and excitation energies $E_{exc,FRS-IC}$ of the $(1/2)^-$ and $(19/2)^+$ isomeric state ^{109n}In. The measured data are compared with the literature values (ME_{Lit}, atomic mass evaluation (AME) [16], and $E_{exc,Lit}$, the atlas of isomers [42]). In the last column, the difference between the measured and literature values is given. # The values and uncertainties are extrapolations obtained from [43].

sensitivity was recently reported to be sufficient for the discovery of isotopes [48]. The $\left(1/2^-\right)$ isomeric state was measured at a rate of 2 per hour. The high sensitivity, mass resolving power, and dynamic range make the MR-TOF-MS an ideal tool to measure and identify exotic nuclei in their ground and isomeric states.

The masses of the ground and $(1/2)^-$ isomeric states of the odd nuclides $^{103-109}$In were determined, as seen in Table 1. In this isotopic chain, all odd isotopes have a $9/2^+$ ground state and a $1/2^-$ isomeric state [16]. The mass excess values are in good agreement with previous storage ring and Penning trap measurements [49, 50]. The results for the excitation energies are in good agreement with previous experiments [51].

The measured mass-to-charge spectrum of $^{97}Ag^+$ ions is shown in Fig. 2. Ground and isomeric states are fitted with a double hyper-EMG [44] (red line for $^{97g}Ag^+$ and blue line for $^{97m}Ag^+$), with one exponential tail on both sides. The peak shape was determined from a high statistical peak. For the isomeric state, 14 counts were detected. The background in the spectrum was measured at 1 count per 3 FWHM. The mass excess values of the ground state was determined to be -70904(12) keV. Previously, the $\left(9/2^+\right)$ ground state of ^{97}Ag was measured indirectly by γ-spectroscopy [52]. The first direct mass measurement is reported in the current paper. The uncertainty of the mass value was reduced by almost an order of magnitude.

For the $\left(1/2^-\right)$ isomeric state, an excitation energy of 618(38) keV was determined from the mass measurement. Recently, new information was added to the level scheme [53]. The measurement of the excitation energy now allows the correct positioning of the negative parity states, i.e., the $\left(3/2^-\right)$ state had an energy of 1853(57) keV, and therefore, above the second $\left(9/2^+\right)$ state.

The nucleus ^{97}Ag was produced in fragmentation, with a production cross section of 1.2 μbarn [47]. An isomer-to-ground state ratio of 0.078 ± 0.005 was measured, corresponding to an effec-

tive production cross section of approximately 90 nbarn for the isomeric state.

The decay properties of ^{97}Ag were investigated in β-delayed γ-spectroscopy, and shell model calculations were performed [54]. The decay properties and with this, the half-life of the $\left(1/2^{-}\right)$ state crucially depends on its excitation energy. Assuming an excitation energy of approximately 600 keV, de-excitation would be only possible via an M4 transition to the ground state, or a Gamow-Teller decay, leading to a predicted half-life up to several hundred seconds. This is in agreement with our expectations, based on the measured extraction time from the CSC of approximately 200 ms, because the isomeric state survived the transport to the MR-TOF-MS. The isomer-to-ground state ratio for the $\left(1/2^{-}\right)$ isomeric state of ^{101}In was measured to be approximately a factor of 2 larger. If we assume a similar ratio for ^{97}Ag, we can concluded that the half-life of ^{97m}Ag should be approximately 200 ms.

The measured masses provide information on the evolution of the mass excess values, in the region below the double magic nucleus ^{100}Sn. From the mass measurement of ^{97}Ag and ^{101}In, the Q_α-value of ^{101}In was directly measured for the first time at -56(23) keV. The extrapolated value stated in the AME [16] was -210(220) keV. Due to the reduction of the error by an order of magnitude, an energetically possible α-decay can now be excluded with a two-sigma confidence-level. In addition, the Q_α-values of ^{105}Sb were directly determined to be 2095(30) keV and the error for ^{97}Ag has been reduced, approximately by an order of magnitude, to -4317(13) keV. These three Q_α-values are necessary for the rp-process calculations [45].

4. Theoretical Results

A comparison of the measured excitation energies of ^{97}Ag and the odd isotopes of $^{101-109}$In, along the isotonic and isotopic chains, with shell-model calculations, provide interesting results. In particular, new data validates the need to include core excitations across $N = 50$, in the calculations.

For the nuclei in the neighborhood of the doubly-magic spherical ^{100}Sn, the leading mechanism of the decay hindrance is associated with the axial symmetry, resulting from the polarization of the core by a few particles (or holes) on top of the closed main shells at $Z = 50$ and/or $N = 50$. The closed shell structures give rise to the strictly spherical geometry; however, the neighboring nuclei are expected to manifest a competition between the slightly oblate ($\beta_2 < 0$) and prolate ($\beta_2 > 0$) quadrupole deformations. Such shape distortions can be described using the nuclear mean-field approach.

4.1. Shell Model Calculation

The evolution of the proton $p_{1/2}$ and $g_{9/2}$ single-hole energies was studied using various shell model (SM) approaches, and compared to the experimental results.

For the $N = 50$ isotones, an empirically determined isospin-asymmetric interaction (GF) [55] was used in a $\pi\nu\left(p_{1/2}, g_{9/2}\right)$ model space, outside a hypothetical ^{76}Sr core. Two-body matrix elements (TBME) and single particle energies (SPE) were fitted to energy spectra and binding energies in $N, Z \leq 50$ nuclei.

The theory is in agreement with the measured data for the $N = 50$ isotones, as seen in Fig. 3. As a result of the first measurement of the ^{97}Ag $(1/2)^{-}$ state, a reliable extrapolation of the ^{99}In value was possible. The extrapolation of the ^{99}In was used as an anchor point for further calculations along the indium isotopic chain.

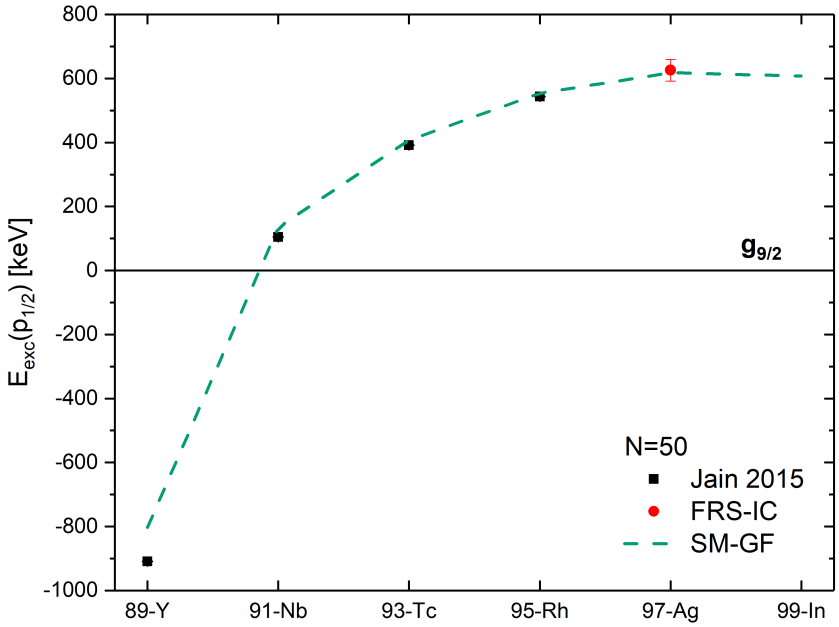

Figure 3: Excitation energy of the $1/2^-$ isomeric state in odd-even $N = 50$ nuclei. The excitation energy measured with the MR-TOF-MS at the FRS Ion Catcher is shown as a red circle. In addition, the values taken from the atlas of nuclear isomers [42] are shown by black squares, and SM-GF calculations [55] by the green dashed line. The ^{89}Y value is negative because it is still in the $\pi p_{1/2}$ sub-shell and $1/2^-$ is the ground state.

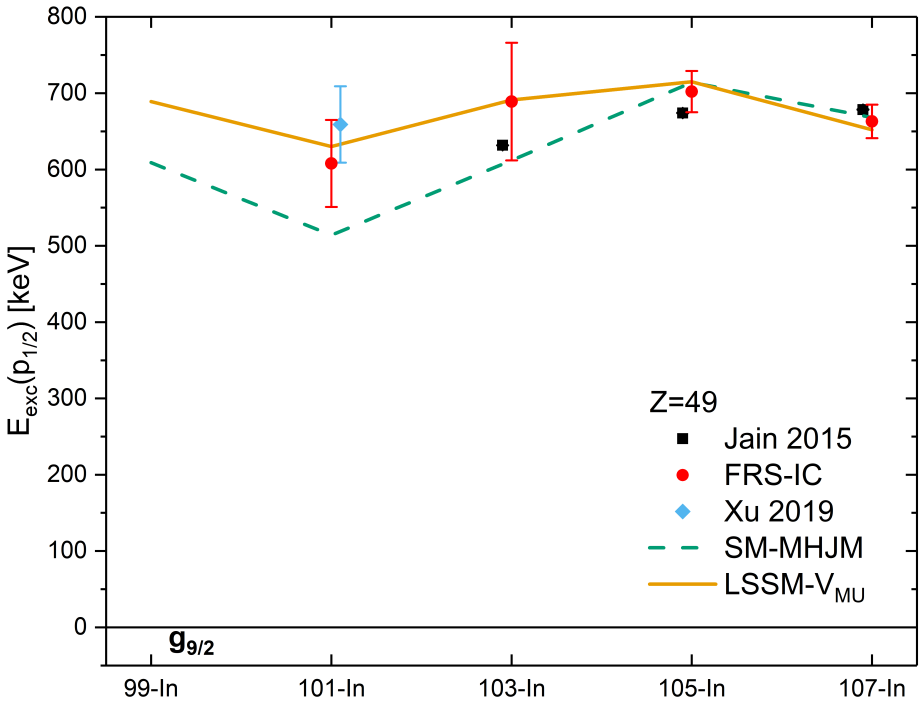

Figure 4: Excitation energy of the $1/2^-$ isomeric state in odd indium nuclei. The excitation energies, measured with the MR-TOF-MS at the FRS Ion Catcher, are indicated by red circles and the values taken from the atlas of nuclear isomers [42], by black squares. The value measured at the HIRFL-CSR facility in Lanzhou [46] is indicated by the blue diamond, SM-MHJM calculations [56], by the green dashed line, and LSSM-V_{MU} calculations [57], by the yellow solid line.

The spectra of $N \geq 50$ In isotopes were calculated in a $\pi\,(p_{1/2}, g_{9/2})\,\nu(g_{7/2}, d_{3/2}, d_{5/2}, s_{1/2}, h_{11/2})$ model space, with an ^{88}Sr core employing a realistic interaction based on a G-matrix, inferred from the charge dependence (CD-Bonn) nucleon-nucleon potential. The interaction was renormalized with respect to the ^{88}Sr SM core, using many-body theory techniques (MHJM) [56], and monopole tuned to reproduce the ^{100}Sn single particle/hole neutron/proton energies [58]. The $\pi\pi$ and $\nu\nu$ TBME were marginally monopole corrected to optimize total binding energies in the $N > 50$ nuclei. It should be noted that in the overlapping $N = 50$ isotones, both approaches yield identical $p_{1/2} - g_{9/2}$ excitation energies.

The $\pi\nu$ interaction results in a kink in the $A = 99 - 101 - 103$ evolution of the excitation energy of the $1/2^-$ state, as can be observed in Fig. 4. This may result from an overestimation of the effect of the $\pi\nu$ interaction for $N > 50$. In the present model space, the $A = 99 - 101$ decrease was due to the strong $\nu g_{7/2} - \pi g_{9/2}$ monopole interaction, as compared to $\nu g_{7/2}\pi p_{1/2}$, which pulled the proton orbitals closer together. The saturation of the excitation energy, up to ^{107}In, was well reproduced.

An inspection of the wave functions indicated that the $1/2^-$ state was dominantly comprised of $\pi p_{1/2}$ coupled to the 0^+ ground state of the Sn isotone; however, in the case of the $9/2^+$ state, coupling to the $2^+ - 8^+$ states was also allowed. The effect of core excitations caused the latter states to increase their excitation, relative to the 0^+ ground state, as known from ^{98}Cd [59] and ^{102}Sn [60].

Therefore, as an alternative to the LSSM approach, core excitations across the $Z, N = 50$ closed shells were included in a $\pi\nu\,(p_{1/2}, g_{9/2})\,\nu\,(g_{7/2}, d_{3/2}, d_{5/2}, s_{1/2}, h_{11/2})$ model space. The interaction was V_{MU} [57] in the $\pi\nu(gdsh)$ space, and was from [61]. The interaction was implemented by $\pi\nu$ V_{MU}, quenched by a factor of 0.75 in the $T = 1$ central force channel. The SPE were chosen to reproduce the present interaction and those of reference [61]. The $p_{1/2}$ SPE in ^{99}In was adjusted to reproduce the general trend. Truncation was applied to allow for up to $3p3h$ excitations across $Z, N = 50$ and $1p1h$ from $(g_{7/2}, d_{5/2})$ to $(d_{3/2}, s_{1/2}, h_{11/2})$. The results showed a relatively flat trend along the indium chain, and a reduced kink for ^{101}In. This was in agreement with the experiment (Fig. 4), and documents the impact of core excitations in low-lying, dominantly single hole states.

4.2. Mean-field Calculation

Large scale nuclear mean-field calculations have been performed for several nuclei in the discussed region. The calculations employed minimization individually, over the axial deformations of each nuclear particle-hole excited-state energy (the deformations, β_2 and β_4, were used). The choice of the employed mean-field Hamiltonian considers that in contemporary nuclear structure physics, special attention is payed to the control of uncertainties of the modeling, and in particular, of the prediction capacities, of nuclei away from the nuclear areas, which served for the parameter adjustments (as seen in [63–66]). For reasons discussed in some detail in [67–70], the phenomenological Woods-Saxon Hamiltonian was chosen, with the universal parameterization of its potential. With a single set of parameters, it describes, on average, all the individual-nucleonic energy levels in nuclei, throughout the chart of nuclides; the relevant information is summarized in [71].

This section is limited to illustrating just a few selected results from the large-scale mean-field calculations addressing K-isomerism in the nuclear mass region, discussed in an upcoming article [72]. The results presented below are parameter-free — no readjustments, related to either the isomers or the excitation spectra in the discussed nuclei, have been performed.

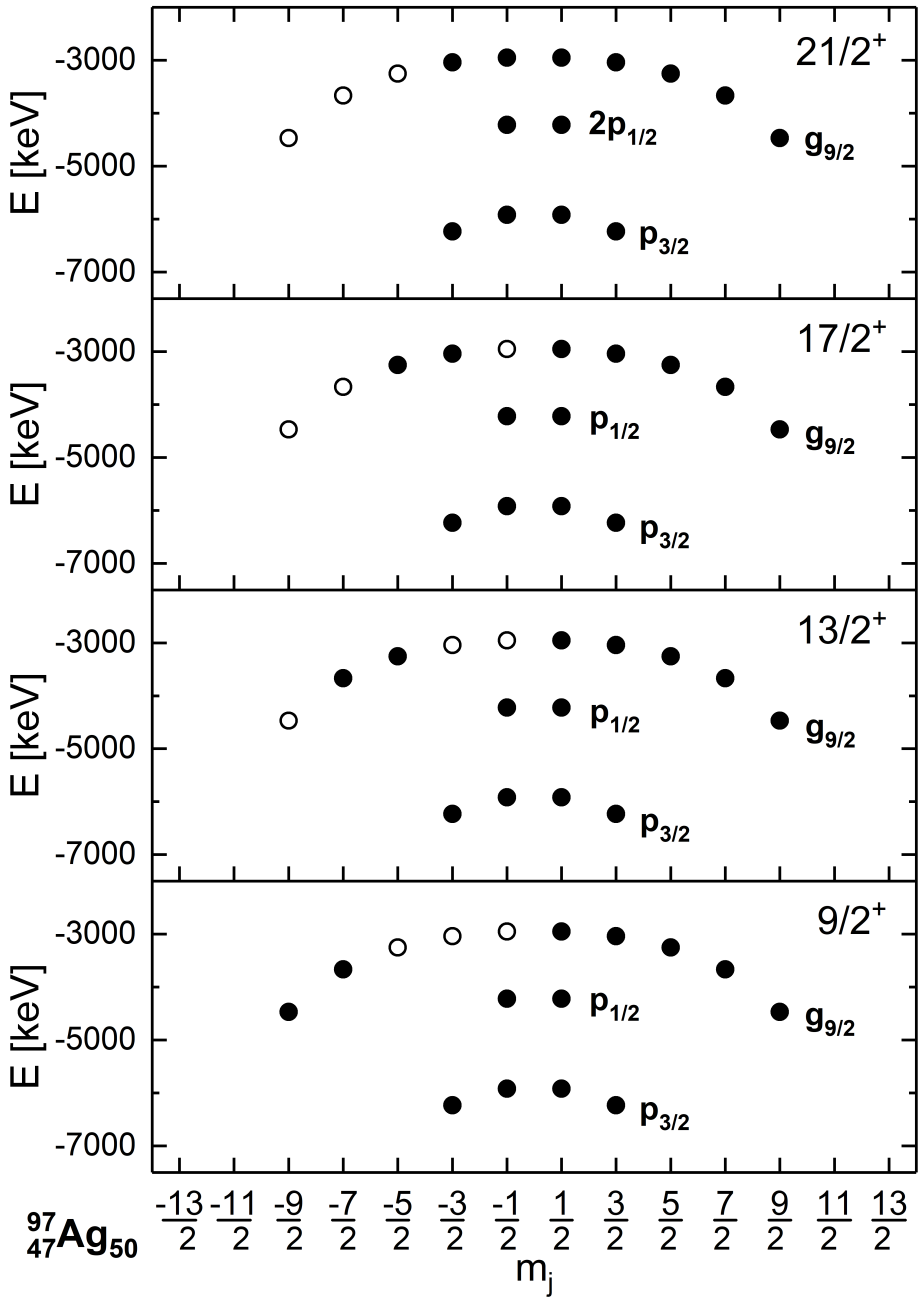

Figure 5: Sequence of deformed mean-field proton configurations (proton single particle levels dependent on the angular momentum projections m_j) corresponding to the maximum alignment state $I^\pi = 21/2^+$ and the other states, which can be connected to it via non-collective E2-transitions, down to the ground-state at $I^\pi = 9/2^+$. Full circles represent the occupied orbitals; open circles, the un-occupied orbitals. All the orbitals, down to the bottom of the potential well (not shown in the figure), were presumed occupied. A deformation of $\beta_2 = -0.09$ and $\beta_4 = +0.02$ were used.

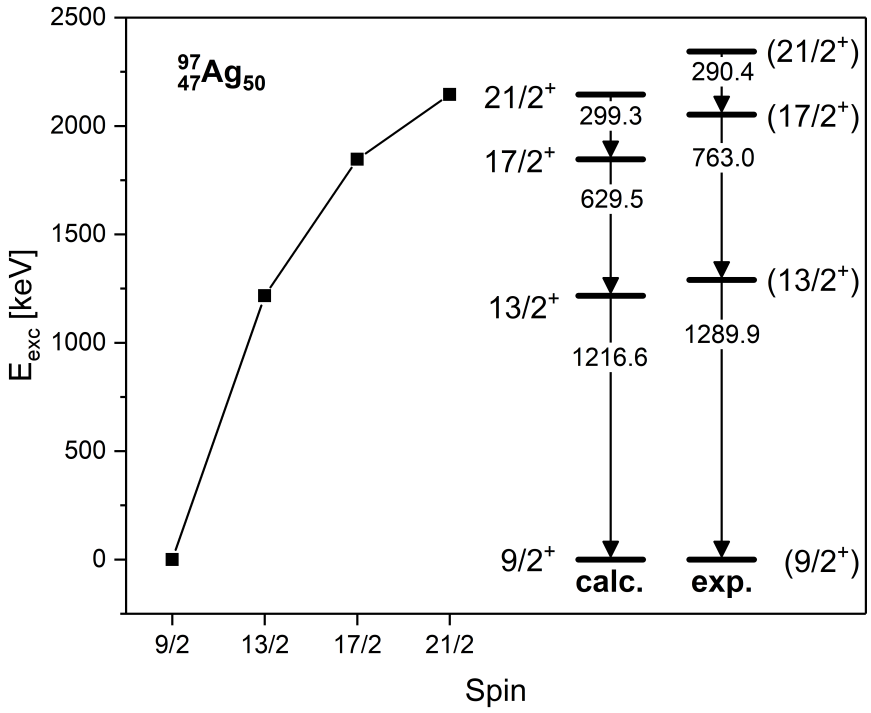

Figure 6: Comparison between the calculated energies of the $I^{\pi} = 9/2^{+}, 13/2^{+}, 17/2^{+}$, and $21/2^{+}$ sequence, discussed in the text (with regard to the calculations). The experimental data was obtained from the National Nuclear Data Center database [62]. A close correspondence of the two sequences can be observed, at the slightly oblate quadrupole deformation, as indicated in the field of Fig. 5.

In constructing the nuclear spectra, with the help of mean-field theory, the maximum-alignment configurations are significant, usually located at or close to, the yrast lines (the term "alignment" relates to the nucleonic angular momenta). An effective approach to finding these lowest energy configurations has been proposed by the Copenhagen School, and is known in the literature as the "tilted Fermi surface method" [73–75]. One of the by-products of the tilted Fermi surface approach are the diagrams, similar to those in Fig. 5, which display the single-nucleon energy positions versus angular momentum projections. They also allow a qualitative discussion on the structures of the configurations, and the varying quadrupole or higher multipolarity axial deformation.

With the help of the aforementioned diagrams, some quantitative or semi-quantitative predictions were formulated in a simple, pedagogical manner. For example, the spin-parity characteristics of the ground-state must be $I^{\pi} = 9/2^{+}$, because the proton orbital closest to the Fermi level in ${}^{97}_{47}\mathrm{Ag}_{50}$ is $1g_{9/2}$. According to the distribution of the mean-field proton orbitals, shown in Fig. 5, an illustration, which is characteristic to the maximum alignment analyses, inherent to the tilted-Fermi-surface method, can be given. There were 6 protons placed in pairwise antiparallel-spin orbitals, with spin projections denoted $\pm m_j$, the seventh one giving rise to the actual value of the ground-state spin (Fig. 12 and 33–35 of [75]).

The lowest energy solutions, obtained with the tilted-Fermi-surface algorithm, often give rise to the yrast-trap configurations and related isomers (Fig. 32 in [75] and references therein).

The maximum alignment configuration possible, without breaking the $Z = 50$ core, using the tilted-Fermi-surface approach, was $I^{\pi}_{max} = 21/2$. A sequence of low-lying positive parity states, with spins satisfying $9/2 < I < 21/2$, corresponding to different placements of the protons within the $1g_{9/2}$ configuration, were simultaneously pedagogically constructed. Some of these states are represented in Fig. 5.

Moreover, there exist low-energy excited states, characterized by $(1/2)^{-}$ that were obtained by promoting one of the protons residing in the $2p_{1/2}$ orbital, and occupying one of the three empty states of $1g_{9/2}$. Because the mean-field calculations showed that transitions de-exciting those latter states are of the type $\Delta I = 4$ or higher, and required a parity change, it was expected that such states would form long-living isomers.

The energies of the characteristic "inverted parabola" sequence, composed of configurations from Fig. 5, were compared to the presently known experimental data in Fig. 6. Because there was no intervention of parameter adjustments, the correspondence can be considered satisfactory, providing confidence in the underlying mean-field algorithm and its more advanced applications, which are not discussed here because it is outside the scope of the paper. The correspondence particularly provides the possibility of formulating some semi-qualitative conclusions about the nature of the $\left(1/2^{-}\right)$ isomer. Within the mean-field interpretation, and depending on which member of the $1g_{9/2}$ orbital is occupied by the proton originating from the $2p_{1/2}$, calculations suggested that there may exist several structures with 8 protons on $1g_{9/2}$, giving rise to a sequence of energies centered about the average position $E^{1/2}_{aver.} \approx 0.6$ MeV, within a ± 0.4 MeV interval. This estimate corresponded satisfactorily, to our experimental findings, at least on the semi-quantitative level.

5. Summary

The first discovery of a nuclear isomeric state, by multiple-reflection time-of-flight mass spectrometry, was achieved by measuring the $\left(1/2^{-}\right)$ isomeric state in ^{97}Ag. The excitation ener-

gies of the $\left(1/2^{-}\right)$ isomeric states in the isotopes ^{97}Ag and $^{101-109}$In were determined from direct mass measurements of the ground and isomeric states of these isotopes, at the FRS Ion Catcher, involving cross sections as low as approximately 30 nbarn. The excitation energy of the $\left(1/2^{-}\right)$ isomeric state in ^{97}Ag was determined to be 618(38) keV. For ^{109}In, a second isomeric state was measured, the half-life of which was only 209 ms. In order to resolve the low-lying isomeric states, the MR-TOF-MS was operated with a mass resolving power of up to 450,000 at a duty cycle of 20 ms. Moreover, the mass of ^{101}In was measured for the first time, and the measurement of the ^{97}Ag ground state mass was improved by more than an order of magnitude. These results showed that the MR-TOF-MS of the FRS Ion Catcher is an efficient tool for discovery of isomeric states, with half-lives in the millisecond range, which is not well studied because of difficulty to access using existing techniques.

The measured excitation energies were compared with shell-model calculations, indicating the need to include core excitations to describe the excitation energies of the $1/2^{-}$ isomeric states along the Indium chain. Furthermore, results obtained within the mean-field approach for the nucleus ^{97}Ag were shown, allowing a better understanding of the level scheme from the "universal parametrization" point of view, and supporting the discovery of the isomeric state in ^{97}Ag.

Acknowledgments

The authors would like to thank A. Kankainen and H. Schatz for fruitful discussions. This work was supported by the German Federal Ministry for Education and Research (BMBF) under contracts no. 05P12RGFN8, 05P16RGFN1, and 05P19RGFN1, by Justus-Liebig-Universität Gießen and GSI under the JLU-GSI strategic Helmholtz partnership agreement, by HGS-HIRe, by the Hessian Ministry for Science and Art (HMWK) through the LOEWE Center HICforFAIR and partially by the Polish National Science Centre under Contract No. 2016/21/B/ST2/01227.

[1] P. Walker, G. Dracoulis, Energy traps in atomic nuclei, Nature 399 (6731) (1999) 35–40.

[2] G. D. Dracoulis, P. M. Walker, F. G. Kondev, Review of metastable states in heavy nuclei, Reports on Progress in Physics 79 (2016) 076301.

[3] A. Aprahamian, Y. Sun, Nuclear physics - Long live isomer research, Nature Physics 1 (2) (2005) 81–82.

[4] R. Schneider, J. Friese, J. Reinhold, K. Zeitelhack, T. Faestermann, R. Gernhäuser, H. Gilg, F. Heine, J. Homolka, P. Kienle, H. J. Körner, H. Geissel, G. Münzenberg, K. Sümmerer, Production and identification of ^{100}Sn, Zeitschrift für Physik A 348 (4) (1994) 241–242.

[5] M. Lewitowicz, R. Anne, G. Auger, D. Bazin, C. Borcea, V. Borrel, J. M. Corre, T. Dörfler, A. Fomichov, R. Grzywacz, D. Guillemaud-Mueller, R. Hue, M. Huyse, Z. Janas, H. Keller, S. Lukyanov, A. C. Mueller, Y. Penionzhkevich, M. Pfützner, F. Pougheon, K. Rykaczewski, M. Saint-Laurent, K. Schmidt, W. Schmidt-Ott, O. Sorlin, J. Szerypo, O. Tarasov, J. Wauters, J. Zylicz, Identification of the doubly-magic nucleus 100Sn in the reaction 112Sn+natNi at 63 MeV/nucleon, Phys. Lett. B 332 (1) (1994) 20 – 24.

[6] T. Faestermann, M. Gorska, H. Grawe, The structure of Sn-100 and neighbouring nuclei, Progress in Particle and Nuclear Physics 69 (2013) 85–130.

[7] I. Čeliković, M. Lewitowicz, R. Gernhäuser, R. Krücken, S. Nishimura, H. Sakurai, D. Ahn, H. Baba, B. Blank, A. Blazhev, P. Boutachkov, F. Browne, G. de France, P. Doornenbal, T. Faestermann, Y. Fang, N. Fukuda, J. Giovinazzo, N. Goel, M. Górska, S. Ilieva, N. Inabe, T. Isobe, A. Jungclaus, D. Kameda, Y.-K. Kim, Y. K. Kwon, I. Kojouharov, T. Kubo, N. Kurz, G. Lorusso, D. Lubos, K. Moschner, D. Murai, I. Nishizuka, J. Park, Z. Patel, M. Rajabali, S. Rice, H. Schaffner, Y. Shimizu, L. Sinclair, P.-A. Söderström, K. Steiger, T. Sumikama, H. Suzuki, H. Takeda, Z. Wang, H. Watanabe, J. Wu, Z. Xu, New Isotopes and Proton Emitters–Crossing the Drip Line in the Vicinity of ^{100}Sn, Phys. Rev. Lett. 116 (2016) 162501.

[8] H. Suzuki, T. Kubo, N. Fukuda, N. Inabe, D. Kameda, H. Takeda, K. Yoshida, K. Kusaka, Y. Yanagisawa, M. Ohtake, H. Sato, Y. Shimizu, H. Baba, M. Kurokawa, K. Tanaka, O. B. Tarasov, D. Bazin, D. J. Morrissey, B. M. Sherrill, K. Ieki, D. Murai, N. Iwasa, A. Chiba, Y. Ohkoda, E. Ideguchi, S. Go, R. Yokoyama, T. Fujii, D. Nishimura, H. Nishibata, S. Momota, M. Lewitowicz, G. DeFrance, I. Celikovic, K. Steiger, Discovery of new isotopes ^{81,82}Mo and ^{85,86}Ru and a determination of the particle instability of ^{103}Sb, Phys. Rev. C 96 (2017) 034604.

[9] K. Auranen, D. Seweryniak, M. Albers, A. D. Ayangeakaa, S. Bottoni, M. P. Carpenter, C. J. Chiara, P. Copp, H. M. David, D. T. Doherty, J. Harker, C. R. Hoffman, R. V. F. Janssens, T. L. Khoo, S. A. Kuvin, T. Lauritsen, G. Lotay, A. M. Rogers, J. Sethi, C. Scholey, R. Talwar, W. B. Walters, P. J. Woods, S. Zhu, Superallowed α Decay to Doubly Magic ^{100}Sn, Phys. Rev. Lett. 121 (2018) 182501.

[10] G. Häfner, K. Moschner, A. Blazhev, P. Boutachkov, P. Davies, R. Wadsworth, F. Ameil, H. Baba, T. Bäck, M. Dewald, et al., Properties of γ-decaying isomers in the Sn 100 region populated in fragmentation of a Xe 124 beam, Phys. Rev. C 100 (2) (2019) 024302.

[11] C. Scheidenberger, The contribution of precision mass measurements to nuclear physics, Nucl. Phys.s A 751 (2005) 209–225.

[12] C. Weber, V.-V. Elomaa, R. Ferrer, C. Fröhlich, D. Ackermann, J. Äystö, G. Audi, L. Batist, K. Blaum, M. Block, A. Chaudhuri, M. Dworschak, S. Eliseev, T. Eronen, U. Hager, J. Hakala, F. Herfurth, F. P. Heßberger, S. Hofmann, A. Jokinen, A. Kankainen, H.-J. Kluge, K. Langanke, A. Martin, G. Martinez-Pinedo, M. Mazzocco, I. D. Moore, J. B. Neumayr, Y. N. Novikov, H. Penttilä, W. R. Plaß, A. V. Popov, S. Rahaman, T. Rauscher, C. Rauth, J. Rissanen, D. Rodriguez, A. Saastamoinen, C. Scheidenberger, L. Schweikhard, D. M. Seliverstov, T. Sonoda, F. K. Thielemann, P. G. Thirolf, G. K. Vorobjev, Mass measurements in the vicinity of the r p-process and the nu p-process paths with the Penning trap facilities JYFLTRAP and SHIPTRAP, Physical Review C 78 (5) (2008) 054310.

[13] V.-V. Elomaa, G. K. Vorobjev, A. Kankainen, L. Batist, S. Eliseev, T. Eronen, J. Hakala, A. Jokinen, I. D. Moore, Y. N. Novikov, H. Penttila, A. Popov, S. Rahaman, J. Rissanen, A. Saastamoinen, H. Schatz, D. M. Seliverstov, C. Weber, J. Aysto, Quenching of the SnSbTe Cycle in the rp Process, Phys. Rev. Lett. 102 (25) (2009) 252501.

[14] M. Breitenfeldt, G. Audi, D. Beck, K. Blaum, S. George, F. Herfurth, A. Herlert, A. Kellerbauer, H. J. Kluge, M. Kowalska, D. Lunney, S. Naimi, D. Neidherr, H. Schatz, S. Schwarz, L. Schweikhard, Penning trap mass measurements of $^{99-109}$Cd with the ISOLTRAP mass spectrometer, and implications for the rp process, Physical Review C 80 (3) (2009) 035805.

[15] E. Haettner, D. Ackermann, G. Audi, K. Blaum, M. Block, S. Eliseev, T. Fleckenstein, F. Herfurth, F. P. Heßberger, S. Hofmann, J. Ketelaer, J. Ketter, H.-J. Kluge, G. Marx, M. Mazzocco, Y. N. Novikov, W. R. Plaß, S. Rahaman, T. Rauscher, D. Rodriguez, H. Schatz, C. Scheidenberger, L. Schweikhard, B. Sun, P. G. Thirolf, G. Vorobjev, M. Wang, C. Weber, Mass Measurements of Very Neutron-Deficient Mo and Tc Isotopes and Their Impact on rp Process Nucleosynthesis, Phys. Rev. Lett. 106 (12) (2011) 122501.

[16] M. Wang, G. Audi, F. G. Kondev, W. J. Huang, S. Naimi, X. Xu, The AME2016 atomic mass evaluation (II). Tables, graphs and references, Chinese Phys. C 41 (3) (2017) 030003.

[17] D. Lubos, J. Park, T. Faestermann, R. Gernhäuser, R. Krücken, M. Lewitowicz, S. Nishimura, H. Sakurai, D. S. Ahn, H. Baba, B. Blank, A. Blazhev, P. Boutachkov, F. Browne, I. Čeliković, G. de France, P. Doornenbal, Y. Fang, N. Fukuda, J. Giovinazzo, N. Goel, M. Górska, S. Ilieva, N. Inabe, T. Isobe, A. Jungclaus, D. Kameda, Y. K. Kim, I. Kojouharov, T. Kubo, N. Kurz, Y. K. Kwon, G. Lorusso, K. Moschner, D. Murai, I. Nishizuka, Z. Patel, M. M. Rajabali, S. Rice, H. Schaffner, Y. Shimizu, L. Sinclair, P.-A. Söderström, K. Steiger, T. Sumikama, H. Suzuki, H. Takeda, Z. Wang, N. Warr, H. Watanabe, J. Wu, Z. Xu, Improved Value for the Gamow-Teller Strength of the ^{100}Sn Beta Decay, Phys. Rev. Lett. 122 (2019) 222502.

[18] R. Wallace, S. E. Woosley, Explosive hydrogen burning, The Astrophysical Journal Supplement Series 45 (1981) 389–420.

[19] H. Schatz, A. Aprahamian, V. Barnard, L. Bildsten, A. Cumming, M. Ouellette, T. Rauscher, F.-K. Thielemann, M. Wiescher, End point of the rp process on accreting neutron stars, Phys. Rev. Lett. 86 (16) (2001) 3471.

[20] B. Sun, Y. A. Litvinov, P. M. Walker, K. Beckert, P. Beller, F. Bosch, D. Boutin, C. Brandau, L. Chen, C. Dimopoulou, H. Geissel, R. Knöbel, C. Kozhuharov, J. Kurcewicz, S. A. Litvinov, M. Mazzocco, J. Meng, C. Nociforo, F. Nolden, W. R. Plass, C. Scheidenberger, M. Steck, H. Weick, M. Winkler, Discovery of a new long-lived isomeric state in ^{125}Ce, The European Physical Journal A 31 (3) (2007) 393–394.

[21] L. Chen, Investigation of stored neutron-rich nuclides in the element range of Pt U with the FRS-ESR facility at 360 400 MeV/u, Ph.D. thesis, Universität Gießen, 2008.

[22] M. Block, C. Bachelet, G. Bollen, M. Facina, C. M. Folden, C. Guénaut, A. A. Kwiatkowski, D. J. Morrissey, G. K. Pang, A. Prinke, R. Ringle, J. Savory, P. Schury, S. Schwarz, Discovery of a Nuclear Isomer in ^{65}Fe with PenningTrap Mass Spectrometry, Phys. Rev. Lett. 100 (2008) 132501.

[23] T. Dickel, W. R. Plaß, A. Becker, U. Czok, H. Geissel, E. Haettner, C. Jesch, W. Kinsel, M. Petrick, C. Scheidenberger, A. Simon, M. I. Yavor, A high-performance multiple-reflection time-of-flight mass spectrometer and isobar separator for the research with exotic nuclei, Nucl. Instrum. Methods A 777 (2015) 172–188.

[24] W. R. Plaß, T. Dickel, C. Scheidenberger, Multiple-reflection time-of-flight mass spectrometry, Int. J. of Mass Spectrom. 349 - 350 (2013) 134 – 144.

[25] W. R. Plaß, T. Dickel, S. Purushothaman, P. Dendooven, H. Geissel, J. Ebert, E. Haettner, C. Jesch, M. Ranjan, M. P. Reiter, H. Weick, F. Amjad, S. Ayet San Andrés, M. Diwisch, A. Estrade, F. Farinon, F. Greiner, N. Kalantar-Nayestanaki, R. Knöbel, J. Kurcewicz, J. Lang, I. Moore, I. Mukha, C. Nociforo, M. Petrick, M. Pfützner, S. Pietri,

A. Prochazka, A.-K. Rink, S. Rinta-Antila, D. Schäfer, C. Scheidenberger, M. Takechi, Y. K. Tanaka, J. S. Winfield, M. I. Yavor, The FRS Ion Catcher - A facility for high-precision experiments with stopped projectile and fission fragments, Nucl. Instrum. Methods B 317 (2013) 457–462.

[26] H. Geissel, P. Armbruster, K. Behr, A. Brünle, K. Burkard, M. Chen, H. Folger, B. Franczak, H. Keller, O. Klepper, B. Langenbeck, F. Nickel, E. Pfeng, M. Pfützner, E. Roeckl, K. Rykaczewski, I. Schall, D. Schardt, C. Scheidenberger, K.-H. Schmidt, A. Schröter, T. Schwab, K. Sümmerer, M. Weber, G. Münzenberg, T. Brohm, H.-G. Clerc, M. Fauerbach, J.-J. Gaimard, A. Grewe, E. Hanelt, B. Knödler, M. Steiner, B. Voss, J. Weckenmann, C. Ziegler, A. Magel, H. Wollnik, J. Dufour, Y. Fujita, D. Vieira, B. Sherrill, The GSI projectile fragment separator (FRS): a versatile magnetic system for relativistic heavy ions, Nucl. Instrum. Methods B 70 (1-4) (1992) 286 – 297.

[27] M. Ranjan, S. Purushothaman, T. Dickel, H. Geissel, W. R. Plaß, D. Schäfer, C. Scheidenberger, J. V. de Walle, H. Weick, P. Dendooven, New stopping cell capabilities: RF carpet performance at high gas density and cryogenic operation, Europhys. Lett. 96 (5) (2011) 52001.

[28] S. Purushothaman, M. P. Reiter, E. Haettner, P. Dendooven, T. Dickel, H. Geissel, J. Ebert, C. Jesch, W. R. Plaß, M. Ranjan, H. Weick, F. Amjad, S. Ayet San Andrés, M. Diwisch, A. Estrade, F. Farinon, F. Greiner, N. Kalantar-Nayestanaki, R. Knöbel, J. Kurcewicz, J. Lang, I. D. Moore, I. Mukha, C. Nociforo, M. Petrick, M. Pfützner, S. Pietri, A. Prochazka, A.-K. Rink, S. Rinta-Antila, C. Scheidenberger, M. Takechi, Y. K. Tanaka, J. S. Winfield, M. I. Yavor, First experimental results of a cryogenic stopping cell with short-lived, heavy uranium fragments produced at 1000 MeV/u, Europhys. Lett. 104 (4) (2013) 42001.

[29] M. Ranjan, P. Dendooven, S. Purushothaman, T. Dickel, M. Reiter, S. Ayet San Andrés, E. Haettner, I. Moore, N. Kalantar-Nayestanaki, H. Geissel, W. Plaß, D. Schäfer, C. Scheidenberger, F. Schreuder, H. Timersma, J. V. de Walle, H. Weick, Design, construction and cooling system performance of a prototype cryogenic stopping cell for the Super-FRS at FAIR, Nucl. Instrum. Methods A 770 (Supplement C) (2015) 87 – 97.

[30] M. P. Reiter, Pilot experiments with relativistic uranium projectile and fission fragments thermalized in a cryogenic gas-filled stopping cell, Ph.D. thesis, Universität Gießen, 2015.

[31] M. P. Reiter, Simulation of the cryogenic stopping cell of the FRS Ion Catcher experiment and construction of a novel RFQ beam line system, Master thesis, Universität Gießen, 2011.

[32] I. Miskun, M. P. Reiter, A. Rink, T. Dickel, S. Ayet San Andrés, J. Ebert, H. Geissel, F. Greiner, E. Haettner, C. Hornung, W. R. Plaß, S. Purushothaman, C. Scheidenberger, An RFQ based beam line and mass filter to improve identification capabilities at the diagnostics unit of the prototype CSC for the LEB, GSI Sci. Rep. 2014 2015-1 (2015) 146 p.

[33] E. Haettner, W. R. Plaß, U. Czok, T. Dickel, H. Geissel, W. Kinsel, M. Petrick, T. Schäfer, C. Scheidenberger, A versatile triple radiofrequency quadrupole system for cooling, mass separation and bunching of exotic nuclei, Nucl. Inst. Methods A 880 (2018) 138–151.

[34] W. R. Plaß, T. Dickel, U. Czok, H. Geissel, M. Petrick, K. Reinheimer, C. Scheidenberger, M. Yavor, Isobar separation by time-of-flight mass spectrometry for low-energy radioactive ion beam facilities, Nucl. Instrum. Methods B 266 (19-20) (2008) 4560–4564.

[35] T. Dickel, Design and Commissioning of an Ultra-High-Resolution Time-of-Flight Based Isobar Separator and Mass Spectrometer, Ph.D. thesis, Universität Gießen, 2010.

[36] H. Geissel, T. Schwab, P. Armbruster, J. P. Dufour, E. Hanelt, K.-H. Schmidt, B. Sherrill, G. Münzenberg, Ions penetrating through ion-optical systems and matterNon-liouvillian phase-space modelling, Nuclear Instruments and Methods in Physics Research Section A 282 (1) (1989) 247–260.

[37] I. Miskun, T. Dickel, I. Mardor, C. Hornung, D. Amanbayev, S. Ayet San Andrés, J. Bergmann, J. Ebert, H. Geissel, M. Górska, F. Greiner, E. Haettner, W. R. Plaß, S. Purushothaman, C. Scheidenberger, A.-K. Rink, H. Weick, S. Bagchi, P. Constantin, S. Kaur, W. Lippert, B. Mei, I. Moore, J.-H. Otto, S. Pietri, I. Pohjalainen, A. Prochazka, C. Rappold, M. P. Reiter, Y. K. Tanaka, J. S. Winfield, A novel method for the measurement of half-lives and decay branching ratios of exotic nuclei, Eur. Phys. J. A 55 (9) (2019) 148.

[38] F. Greiner, T. Dickel, S. Ayet San Andrés, J. Bergmann, P. Constantin, J. Ebert, H. Geissel, E. Haettner, C. Hornung, I. Miskun, W. Lippert, I. Mardor, I. Moore, W. R. Plaß, S. Purushothaman, A.-K. Rink, M. P. Reiter, C. Scheidenberger, H. Weick, Removal of molecular contamination in low-energy RIBs by the isolation-dissociation-isolation method, Nucl. Instrum. Methods B, in press .

[39] C. Hornung, High-Resolution Experiments with the Multiple-Reflection Time-Of-Flight Mass Spectrometer at the Fragment Separator FRS, Ph.D. thesis, Universität Gießen, 2018.

[40] S. Ayet San Andrés, C. Hornung, J. Ebert, W. R. Plaß, T. Dickel, H. Geissel, C. Scheidenberger, J. Bergmann, F. Greiner, E. Haettner, C. Jesch, W. Lippert, I. Mardor, I. Miskun, Z. Patyk, S. Pietri, A. Pihktelev, S. Purushothaman, M. P. Reiter, A.-K. Rink, H. Weick, M. I. Yavor, S. Bagchi, V. Charviakova, P. Constantin, M. Diwisch, A. Finlay, S. Kaur, R. Knöbel, J. Lang, B. Mei, I. D. Moore, J.-H. Otto, I. Pohjalainen, A. Prochazka, C. Rappold, M. Takechi, Y. K. Tanaka, J. S. Winfield, X. Xu, High-resolution, accurate multiple-reflection time-of-flight mass spectrometry for short-lived, exotic nuclei of a few events in their ground and low-lying isomeric states, Phys. Rev. C 99 (2019) 064313.

[41] D. Amanbayev, in preparation, Ph.D. thesis, Universität Gießen, 2019.
[42] A. K. Jain, B. Maheshwari, S. Garg, M. Patial, B. Singh, Atlas of nuclear isomers, Nucl. Data Sheets 128 (2015) 1–130.
[43] G. Audi, F. G. Kondev, M. Wang, W. J. Huang, S. Naimi, The NUBASE2016 evaluation of nuclear properties, Chinese Phys. C 41 (3) (2017) 030001.
[44] S. Purushothaman, S. Ayet San Andrés, J. Bergmann, T. Dickel, J. Ebert, H. Geissel, C. Hornung, W. R. Plaß, C. Rappold, C. Scheidenberger, Y. K. Tanaka, M. I. Yavor, Hyper-EMG: A new probability distribution function composed of Exponentially Modified Gaussian distributions to analyze asymmetric peak shapes in high-resolution time-of-flight mass spectrometry, Int. J. Mass Spectrom. 421 (2017) 245–254.
[45] H. Schatz, W.-J. Ong, Dependence of X-ray burst models on nuclear masses, The Astrophysical Journal 844 (2) (2017) 139.
[46] X. Xu, J. H. Liu, C. X. Yuan, Y. M. Xing, M. Wang, Y. H. Zhang, X. H. Zhou, Y. A. Litvinov, K. Blaum, R. J. Chen, X. C. Chen, C. Y. Fu, B. S. Gao, J. J. He, S. Kubono, Y. H. Lam, H. F. Li, M. L. Liu, X. W. Ma, P. Shuai, M. Si, M. Z. Sun, X. L. Tu, Q. Wang, H. S. Xu, X. L. Yan, J. C. Yang, Y. J. Yuan, Q. Zeng, P. Zhang, X. Zhou, W. L. Zhan, S. Litvinov, G. Audi, S. Naimi, T. Uesaka, Y. Yamaguchi, T. Yamaguchi, A. Ozawa, B. H. Sun, K. Kaneko, Y. Sun, F. R. Xu, Masses of ground and isomeric states of ^{101}In and configuration-dependent shell evolution in odd-A indium isotopes, arXiv preprint arXiv:1907.04584 .
[47] H. Suzuki, T. Kubo, N. Fukuda, N. Inabe, D. Kameda, H. Takeda, K. Yoshida, K. Kusaka, Y. Yanagisawa, M. Ohtake, H. Sato, Y. Shimizu, H. Baba, M. Kurokawa, T. Ohnishi, K. Tanaka, O. Tarasov, D. Bazin, D. Morrissey, B. Sherrill, K. Ieki, D. Murai, N. Iwasa, A. Chiba, Y. Ohkoda, E. Ideguchi, S. Go, R. Yokoyama, T. Fujii, D. Nishimura, H. Nishibata, S. Momota, M. Lewitowicz, G. DeFrance, I. Celikovic, K. Steiger, Production cross section measurements of radioactive isotopes by BigRIPS separator at RIKEN RI Beam Factory, Nucl. Instrum. Methods B 317 (2013) 756 – 768.
[48] L. Chen, W. R. Plaß, H. Geissel, R. Knöbel, C. Kozhuharov, Y. A. Litvinov, Z. Patyk, C. Scheidenberger, K. Siegień-Iwaniuk, B. Sun, H. Weick, K. Beckert, P. Beller, F. Bosch, D. Boutin, L. Caceres, J. J. Carroll, D. M. Cullen, I. J. Cullen, B. Franzke, J. Gerl, M. Górska, G. Jones, A. Kishada, J. Kurcewicz, S. Litvinov, Z. Liu, S. Mandal, F. Montes, G. Münzenberg, F. Nolden, T. Ohtsubo, Z. Podolyk, R. Propri, S. Rigby, N. Saito, T. Saito, M. Shindo, M. Steck, P. Ugorowski, P. Walker, S. Williams, M. Winkler, H.-J. Wollersheim, T. Yamaguchi, Discovery and investigation of heavy neutron-rich isotopes with time-resolved Schottky spectrometry in the element range from thallium to actinium, Phys. Lett. B 691 (5) (2010) 234 – 237.
[49] Y. Litvinov, H. Geissel, T. Radon, F. Attallah, G. Audi, K. Beckert, F. Bosch, M. Falch, B. Franzke, M. Hausmann, M. Hellström, T. Kerscher, O. Klepper, H.-J. Kluge, C. Kozhuharov, K. Löbner, G. Münzenberg, F. Nolden, Y. Novikov, W. Quint, Z. Patyk, H. Reich, C. Scheidenberger, B. Schlitt, M. Steck, K. Sümmerer, L. Vermeeren, M. Winkler, T. Winkler, H. Wollnik, Mass measurement of cooled neutron-deficient bismuth projectile fragments with time-resolved Schottky mass spectrometry at the FRS-ESR facility, Nucl. Phys. A 756 (1) (2005) 3 – 38.
[50] A. Martın, D. Ackermann, G. Audi, K. Blaum, M. Block, A. Chaudhuri, Z. Di, S. Eliseev, R. Ferrer, D. Habs, et al., Mass measurements of neutron-deficient radionuclides near the end-point of the rp-process with SHIPTRAP, The European Physical Journal A 34 (4) (2007) 341–348.
[51] J. Szerypo, R. Grzywacz, Z. Janas, M. Karny, M. Pfützner, A. Plochocki, K. Rykaczewski, J. Żylicz, M. Huyse, G. Reusen, J. Schwarzenberg, P. V. Duppen, A. Woehr, H. Keller, R. Kirchner, O. Klepper, A. Piechaczek, E. Roeckl, K. Schmidt, L. Batist, A. Bykov, V. Wittman, B. A. Brown, Decay properties of ground-state and isomer of ^{103}In, Zeitschrift für Physik A Hadrons and Nuclei 359 (2) (1997) 117–126.
[52] Z. Hu, L. Batist, J. Agramunt, A. Algora, B. A. Brown, D. Cano-Ott, R. Collatz, A. Gadea, M. Gierlik, M. Górska, H. Grawe, M. Hellström, Z. Janas, M. Karny, R. Kirchner, F. Moroz, A. Płochocki, M. Rejmund, E. Roeckl, B. Rubio, M. Shibata, J. Szerypo, J. L. Tain, V. Wittmann, β decay of ^{97}Ag: Evidence for the Gamow-Teller resonance near ^{100}Sn, Physical Review C 60 (1999) 024315.
[53] J. Park, R. Krücken, D. Lubos, R. Gernhäuser, M. Lewitowicz, S. Nishimura, D. S. Ahn, H. Baba, B. Blank, A. Blazhev, P. Boutachkov, F. Browne, I. Čeliković, G. de France, P. Doornenbal, T. Faestermann, Y. Fang, N. Fukuda, J. Giovinazzo, N. Goel, M. Górska, H. Grawe, S. Ilieva, N. Inabe, T. Isobe, A. Jungclaus, D. Kameda, G. D. Kim, Y.-K. Kim, I. Kojouharov, T. Kubo, N. Kurz, Y. K. Kwon, G. Lorusso, K. Moschner, D. Murai, I. Nishizuka, Z. Patel, M. M. Rajabali, S. Rice, H. Sakurai, H. Schaffner, Y. Shimizu, L. Sinclair, P.-A. Söderström, K. Steiger, T. Sumikama, H. Suzuki, H. Takeda, Z. Wang, H. Watanabe, J. Wu, Z. Y. Xu, New and comprehensive β- and βp-decay spectroscopy results in the vicinity of ^{100}Sn, Phys. Rev. C 99 (2019) 034313.
[54] K. Schmidt, P. C. Divari, T. W. Elze, R. Grzywacz, Z. Janas, I. P. Johnstone, M. Karny, H. Keller, R. Kirchner, O. Klepper, A. Plochocki, E. Roeckl, K. Rykaczewski, L. D. Skouras, J. Szerypo, J. Zylicz, Decay properties of very neutron-deficient isotopes of Silver and Cadmium, Nuclear Physics A 624 (2) (1997) 185–209.
[55] R. Gross, A. Frenkel, Effective interaction of protons and neutrons in the $2p_{1/2} - 1g_{9/2}$ subshells, Nuclear Physics A 267 (1976) 85–108.
[56] M. Hjorth-Jensen, T. T. S. Kuo, E. Osnes, Realistic effective interactions for nuclear systems, Phys. Rep. 261 (3-4)

(1995) 125–270.
[57] T. Otsuka, T. Suzuki, M. Honma, Y. Utsuno, N. Tsunoda, K. Tsukiyama, M. Hjorth-Jensen, Novel features of nuclear forces and shell evolution in exotic nuclei, Phys. rev. lett. 104 (1) (2010) 012501.
[58] O. Kavatsyuk, C. Mazzocchi, Z. Janas, A. Banu, L. Batist, F. Becker, A. Blazhev, W. Brüchle, J. Döring, T. Faestermann, M. Górska, H. Grawe, A. Jungclaus, M. Karny, M. Kavatsyuk, O. Klepper, R. Kirchner, M. La Commara, K. Miernik, I. Mukha, C. Plettner, A. Płochocki, E. Roeckl, M. Romoli, K. Rykaczewski, M. Schädel, K. Schmidt, R. Schwengner, J. Żylicz, Beta decay of ^{101}Sn, The European Physical Journal A 31 (3) (2007) 319–325.
[59] A. Blazhev, M. Górska, H. Grawe, J. Nyberg, M. Palacz, E. Caurier, O. Dorvaux, A. Gadea, F. Nowacki, C. Andreoiu, G. de Angelis, D. Balabanski, C. Beck, B. Cederwall, D. Curien, J. Döring, J. Ekman, C. Fahlander, K. Lagergren, J. Ljungvall, M. Moszyński, L.-O. Norlin, C. Plettner, D. Rudolph, D. Sohler, K. M. Spohr, O. Thelen, M. Weiszflog, M. Wisell, M. Wolińska, W. Wolski, Observation of a core-excited $E4$ isomer in ^{98}Cd, Physical Review C 69 (6) (2004) 064304.
[60] F. Nowacki, Shell model description of correlations in ^{56}Ni and ^{100}Sn, Nuclear Physics A 704 (1) (2002) 223 – 231, RIKEN Symposium Shell Model 2000.
[61] T. Togashi, Y. Tsunoda, T. Otsuka, N. Shimizu, M. Honma, Novel Shape Evolution in Sn Isotopes from Magic Numbers 50 to 82, Phys. Rev. Lett. 121 (2018) 062501.
[62] N. Nica, Nuclear data sheets for A= 97, Nuclear Data Sheets 111 (3) (2010) 525–716.
[63] J. Dudek, B. Szpak, M.-G. Porquet, H. Molique, K. Rybak, B. Fornal, Nuclear Hamiltonians: the question of their spectral predictive power and the associated inverse problem, Journal of Physics G: Nuclear and Particle Physics 37 (6) (2010) 064031.
[64] J. Dobaczewski, W. Nazarewicz, P. Reinhard, Error estimates of theoretical models: a guide, Journal of Physics G: Nuclear and Particle Physics 41 (7) (2014) 074001.
[65] P. G. Reinhard, Estimating the relevance of predictions from the Skyrme–Hartree–Fock model, Physica Scripta 91 (2) (2015) 023002.
[66] J. Erler, P. G. Reinhard, Error estimates for the Skyrme–Hartree–Fock model, Journal of Physics G: Nuclear and Particle Physics 42 (3) (2015) 034026.
[67] J. Dudek, B. Szpak, M.-G. Porquet, B. Fornal, Statistical significance of theoretical predictions: A new dimension in nuclear structure theories (I), Journal of Physics: Conference Series 267 (2011) 012062.
[68] B. Szpak, J. Dudek, M.-G. Porquet, B. Fornal, Statistical significance of theoretical predictions: A new dimension in nuclear structure theories (II), Journal of Physics: Conference Series 267 (2011) 012063.
[69] I. Dedes, J. Dudek, Predictive power of theoretical modelling of the nuclear mean field: examples of improving predictive capacities, Physica Scripta 93 (4) (2018) 044003.
[70] I. Dedes, J. Dudek, Propagation of the nuclear mean-field uncertainties with increasing distance from the parameter adjustment zone: Applications to superheavy nuclei, Physical Review C 99 (5) (2019) 054310.
[71] S. Cwiok, W. Nazarewicz, J. Dudek, J. Skalski, T. Werner, Single-particle energies, wave functions, quadrupole moments and g-factors in an axially deformed woods-saxon potential with applications to the two-centre-type nuclear problems, Comp. Phys. Comm. 46 (1987) 379.
[72] I. Dedes, et. al, in preparation .
[73] M. Cerkaski, J. Dudek, Z. Szymański, C. G. Andersson, G. Leander, S. Åberg, S. G. Nilsson, I. Ragnarsson, Search for the yrast traps in neutron deficient rare earth nuclei, Physics Letters B 70 (1) (1977) 9–13.
[74] M. Cerkaski, J. Dudek, P. Rozmej, Z. Szymański, S. G. Nilsson, Particle-hole structure of nuclear isomers at high angular momenta, Nuclear Physics A 315 (3) (1979) 269–290.
[75] M. J. A. De Voigt, J. Dudek, Z. Szymański, High-spin phenomena in atomic nuclei, Reviews of Modern Physics 55 (4) (1983) 949.